

First Result for Dark Matter Search by WINERED

Wen Yin¹, Taiki Bessho², Yuji Ikeda^{3,2}, Hitomi Kobayashi², Daisuke Taniguchi⁴,
Hiroaki Sameshima⁵, Noriyuki Matsunaga⁶, Shogo Otsubo³, Yuki Sarugaku³,
Tomomi Takeuchi³, Haruki Kato³, Satoshi Hamano⁴, Hideyo Kawakita^{3,7}

¹*Department of Physics, Tohoku University, Sendai, Miyagi 980-8578, Japan*

²*PhotoCross Co. Ltd., 17-203 Iwakura-Minami-Osagicho, Sakyo-ku, Kyoto 606-0003,
Japan*

³*Laboratory of Infrared High-resolution Spectroscopy,
Koyama Astronomical Observatory, Kyoto Sangyo University
Motoyama, Kamigamo, Kita-ku, Kyoto 603-8555, Japan*

⁴*National Astronomical Observatory of Japan, 2-21-1 Osawa, Mitaka, Tokyo 181-8588,
Japan*

⁵*Institute of Astronomy, the University of Tokyo, 2-21-1 Osawa, Mitaka, Tokyo 181-0015,
Japan*

⁶*Department of Astronomy, Graduate School of Science, University of Tokyo, 7-3-1 Hongo,
Bunkyo-ku, Tokyo 113-0033, Japan*

⁷*Department of Astrophysics and Atmospheric Sciences, Faculty of Science, Kyoto Sangyo
University*

Abstract

The identity of dark matter has been a mystery in astronomy, cosmology, and particle theory for about a century. Bessho, Ikeda, and Yin (2022), three of the current authors, proposed using the state-of-the-art infrared spectrographs, including WINERED at 6.5m Magellan Clay telescope and NIRSpec at James Webb Space Telescope, as efficient detectors for the indirect detection of dark matter with the mass around eV by measuring the line photons from the dark matter two body decays. Applying this concept, we have performed spectrographic observations of dwarf spheroidal galaxies (dSphs) Leo V and Tucana II using WINERED by utilizing an object-sky-object nodding observation technique for background subtraction. We present the first result from this dark matter search. Employing zero consistent flux data after the sky subtraction, we have established one of the most stringent limits to date on dark matter decaying

into line photons in the mass range of $1.8 - 2.7 \text{ eV}$. Our data can also be applied to constrain other spectra of photons from the dSphs.

1 Introduction

Dark Matter has played a crucial role in the evolution of the universe, and its existence is now considered certain in the current universe. Yet, despite numerous experimental searches, the basic properties of dark matter, such as mass and non-gravitational interactions, have remained unknown for about a century. The spatial distribution of dark matter within galaxies is typically inferred from gravitational interactions, evident in phenomena like the rotation curves of galaxies.

One candidate for dark matter is an undiscovered elementary particle known as the axion-like particle (ALP), which couples with photons. Theoretically, scenarios like the “ALP miracle” [1, 2] (see also [3] where the strong CP problem can be explained) and the “hadronic axion window” [4, 5] predict the existence of ALPs with masses near eV. In both scenarios, the dark matter decays into two photons, producing narrow-line emissions in the near-infrared region. Throughout this paper, we refer to narrow-line emissions simply as ‘lines’. By searching for line emission spectra in the near-infrared region, there is a potential to discover eV-range dark matter. In addition, the hot dark matter paradigm, prevalent about 40 years ago, suggests dark matter mass around eV. A similar model can account for cold dark matter in the eV mass range if the Bose-enhancement effect is significant in thermal production [6]. Particularly when the coupling constant between ALP dark matter and photons lies in the range of $g_{\phi\gamma\gamma} = 10^{-11} - 10^{-10} \text{ GeV}^{-1}$, it can explain several analyzed excesses relevant to the cosmic infrared background together if the mass is around 2 eV [7–9](see also [10]). Motivated by these discussions, we will study the search for dark matter decaying into line photons, especially with the mass around 2 eV.

Recently, authors in Ref. [11] proposed that by using the state-of-the-art infrared spectrographs such as Warm INfrared Echelle spectrograph for Realizing Extreme Dispersion and sensitivity (WINERED) installed at the 6.5m Magellan Clay telescope and the Near-Infrared Spectrograph (NIRSpec) at the James Webb Space Telescope (JWST), can efficiently search for the eV range dark matter. This efficiency is particularly relevant if the dark matter decays into a line photon, as background noises usually constitute continuous spectra, making the background appear dark in spectrographs with good spectral resolution. A similar search can be done in the Infrared Camera and Spectrograph (IRCS) installed on the 8.2 m Subaru Telescope. Since the IRCS and WINERED in the telescopes have very good angular resolution and small field-of-view, precise estimations of the angular dependence of the photon flux from the dark matter decay in 35 dSphs were done [12].

In this paper, we use the WINERED [13–18], a near-infrared, high-resolution spectro-

graph developed by the University of Tokyo alongside the Laboratory of Infrared High-resolution Spectroscopy at Kyoto Sangyo University, to search for dark matter. It is a PI-type instrument that began operating with the 3.58m New Technology Telescope (NTT) at La Silla Observatory in 2017 and was subsequently fitted to the 6.5m Magellan Clay telescope at Las Campanas Observatory. Offering unparalleled sensitivity with an instrumental throughput reaching up to 50%, WINERED stands out among near-infrared high-resolution spectrographs, attachable to telescopes ranging from intermediate (3-4m class) to large (8-10m class), especially in the short NIR spectrum (0.9-1.35 μ m). WINERED is equipped with three observational settings: the “WIDE” mode ($R = 28000$), the “HIRES-Y” mode ($R = 68000$), and the “HIRES-J” mode ($R = 68000$). Here $R \equiv \lambda/\Delta\lambda_{\text{FWHM}}$ quantify the spectral resolution with λ ($\Delta\lambda_{\text{FWHM}}$) being the wavelength (peak full width at half of the maximum height).

On July 6th, 2023, we used the “WIDE” mode of WINERED on the Magellan Telescope to perform 1-hour observation of the Leo V dwarf spheroidal galaxy (dSph), and 0.5-hour observation for the blank sky to subtract the background noise to search for dark matter. We found some excesses in the data. One way to further reduce the noise is to examine the Doppler shift in the line wavelength, which arises from the varying radial velocities among different dSphs as suggested in [11]. Therefore, we performed the second observation on November 2nd, 2023, by looking at the Tucana II for 1.2 hours with a blank sky observation of 0.7 hours.

In this paper, we use data consistent with zero after sky subtraction to establish a limit on the dark matter decay rate, assuming that dark matter decays into two particles, one of which is a photon. We find that our observational data can set one of the strongest limits on dark matter decay rate in the mass range of 1.8 – 2.7 eV. Our result is robust because we do not rely on a specific background model. Furthermore, these data enable us to constrain a wide array of photon-producing processes, extending beyond those that produce line signals.

Here, we mention that the dark matter search using the NIRSpec at JWST, as proposed in [11], was performed by analyzing public blank sky data. This search aimed to constrain the decay rate of the dark matter in the Milky-way galaxy, as detailed in Refs. [19] (and [20], which used a more conservative D -factor, defined in Eq. (5)). The background analysis done in [11] is consistent with Refs. [19, 20]. The future reach/sensitivity was also estimated in Refs. [11, 19, 20]. Since the observational targets and methods are different, the constraints are mutually complementary. The limit from this paper will be typically stronger than the ones in previous studies in the mass range of 1.8 – 2.7eV for the model-independent analysis (and also the background-model-dependent analysis unless we adopt a very conservative

differential D -factor of the dSphs).¹ In the optical range, indirect detection of dark matter was also done [21–23] by employing optical spectrographs using real experimental data. Our result is in the complementary mass range.

2 Lines from Dark Matter in dSphs

Our main focus in this paper is the dark matter that decays into two particles, one of which is a photon. Here, we define the decay rate as Γ_ϕ , which also represents the inverse of the lifetime, and denote the number of photons in the final states by q . The mass of the dark matter is m_ϕ . We assume that both daughter particles are significantly lighter than the dark matter and thus neglect their masses. For instance, the well-studied ALP dark matter has $\Gamma_\phi = \frac{g_{\phi\gamma\gamma}^2}{64\pi} m_\phi^3$, where $g_{\phi\gamma\gamma}$ is the ALP coupling to photons, and $q = 2$.

The photon differential flux at the outer surface of the Earth’s atmosphere from this decay comprises two parts,

$$\frac{d\Phi_\gamma}{dE_\gamma} = \frac{d\Phi_\gamma^{\text{extra}}}{dE_\gamma} + \sum_i \frac{d\Phi_{\gamma,i}}{dE_\gamma} \quad (1)$$

where the first term on the right-hand side represents an isotropic extragalactic component with a characteristic energy scaling. We do not consider this component in our analysis as it would induce a continuous spectrum that gives lower sensitivity compared to the second term on the right-hand side. In addition, it will be reduced by the sky subtraction in our analysis.

The second term is our focal point, and we consider the emission from a given nearby galaxy i in the angular direction of Ω . Angular differential flux can be expressed as

$$\frac{\partial^2 \Phi_{\gamma,i}}{\partial \Omega \partial E} = \int ds \frac{e^{-\tau[s,\Omega]s}}{4\pi s^2} \left(\frac{q\Gamma_\phi \rho_\phi^i(s, \Omega)}{m_\phi} \right) s^2 \frac{\partial^2 N_{\phi,i}}{q \partial E \partial \Omega} [s, \Omega] \simeq \frac{\partial_\Omega D[s, \Omega]}{4\pi} \frac{q\Gamma_\phi}{m_\phi} \frac{\partial^2 \bar{N}_{\phi,i}}{q \partial E \partial \Omega}. \quad (2)$$

In this equation, s denotes the line-of-sight distance. ρ_ϕ^i and $\frac{\partial^2 N_{\phi,i}}{q \partial E \partial \Omega} [s, \Omega]$ signify the dark matter density profile and the emission spectrum of each photon from an individual dark matter decay in the vicinity of galaxy i , respectively. Both of the factors are contingent upon the dark matter profile models and the attributes of galaxy i in general. In the approximation, we assume that the dependence on s and Ω in $\partial^2 N_{\phi,i} / \partial E \partial \Omega$ is not significant,

¹We will not perform the model-dependent analysis dubbed as continuum model in Ref. [19], where the authors first fit the data by using smooth spline functions and lines, which are assumed to be not from dark matter. Then, they subtract them from the data and place a limit for the two-body decay rate of the dark matter. This analysis may exclude possible dark matter signal.

and we factorize the integral. Indeed, those decay signals look like lines for the WINERED in the WIDE mode, in which $R = 28000$, given that the typical velocity dispersion of the dark matter in a dSph is smaller than 10km/s. Thus, we can approximate

$$\frac{\partial^2 N_{\phi,i}}{q\partial E\partial\Omega} \simeq \frac{\partial^2 \bar{N}_{\phi,i}}{q\partial E\partial\Omega} = 2\delta\left(E - \frac{m_\phi}{2}(1 - v_i/c)\right) \quad (3)$$

by neglecting the velocity dispersion of the dwarf (see more precise treatment by including them in Ref. [11,12]). However, we do consider the radial velocities of the dSphs since they are much larger. For instance, the radial velocities of Leo V and Tucana II are [24],

$$v_{\text{LeoV}} \approx 173.3 \text{ km/s}, \text{ and } v_{\text{TucII}} \approx -129.1 \text{ km/s}, \quad (4)$$

respectively. The term

$$\partial_\Omega D_i \equiv \int ds \rho_\phi^i \quad (5)$$

is the so-called differential D -factor [25–33], which is carefully derived in [12] as a function of the angle Ω measured from the center of galaxy (see also [34, 35]). For Leo V, $\log_{10}(\partial_\Omega D_{\text{LeoV}}/[\text{GeV}/\text{cm}^2/\text{sr}]) \approx 21.4_{-0.7}^{+0.9}$ around the center of the galaxy in the level of $\mathcal{O}(\text{arcsec})$, which will be the position we look at. For Tucana II, $\log_{10}(\partial_\Omega D_{\text{TucII}}/[\text{GeV}/\text{cm}^2/\text{sr}]) \approx 22.2_{-0.9}^{+1.4}$. Here, we adopted the estimation in Ref. [12]. For Tucana II, the differential D -factor is larger than the conservative one estimated in Ref. [11], in which the typical value of the D -factor around the dSph (but not close to the center) was used. This is because the dark matter around the center is denser than the other regions in the dSph. In particular, Tucana II may have a cuspy profile around the center of the galaxy. We take this possibility into account to estimate the uncertainty. In such a case, the differential D -factor can be enhanced by an order of magnitude compared to the conservative estimation. τ represents the (averaged) optical depth. For the targets and wavelengths of interest, we can neglect the scattering or absorption of the photon during the propagation to the outer surface of Earth’s atmosphere. However, those effects due to the atmosphere of Earth cannot be neglected. To estimate the flux on ground-based telescopes, we simply use

$$\eta(2\pi/E_\gamma) \times \frac{\partial^2 \Phi_{\gamma,i}}{\partial\Omega\partial E_\gamma} \Big|_{\tau=0}, \quad (6)$$

where $\eta[\lambda]$ denotes the atmospheric transmittance, which we will measure from the observation of a standard star by using the software package Molecfit [36,37].

From those discussions and by applying the estimate in Ref. [12],

$$\partial_{\Omega}\Phi_{\gamma,\text{LeoV}} \approx 1.33_{-1.07}^{+8.28} \times 10^{-6} \text{cm}^{-2} \text{s}^{-1} \text{arcsec}^{-2} \left(\frac{2 \text{eV}}{m_{\phi}} \right) \frac{q\Gamma_{\phi}}{(1.65 \times 10^{24} \text{s})^{-1}}, \quad (7)$$

$$\partial_{\Omega}\Phi_{\gamma,\text{TucII}} \approx 9.83_{-8.59}^{+210.14} \times 10^{-6} \text{cm}^{-2} \text{s}^{-1} \text{arcsec}^{-2} \left(\frac{2 \text{eV}}{m_{\phi}} \right) \frac{q\Gamma_{\phi}}{(1.65 \times 10^{24} \text{s})^{-1}}. \quad (8)$$

The flux will be compared with the observational data to set a limit on the dark matter decay rate.

3 Observation and Data Reduction

3.1 Observation

Observations were conducted using the WINERED [38] attached to the 6.5m Magellan Clay telescope on July 6th and November 2nd in 2023. We used the WIDE mode with a 0.29 arcsec slit that allows us to cover the wavelength region of $\lambda = 0.92 - 1.35 \mu\text{m}$ with a spectral resolution of $R = 28,000$. The observation targets were Leo V (on 6th, Jul, 2023) and Tucana II (on 2nd, Nov, 2023), which are dSphs located at a distance of 178 kpc and 57 kpc, respectively. The high-level emission originating from eV dark matter is expected due to the high central concentration of these targets ($\theta_{\text{max}} \sim 0.07^{\circ}$ and $\sim 1.0^{\circ}$), see Ref. [11]. The spectrometer slit (0.29 arcsec \times 8.6 arcsec) was positioned near the optical centroids of dSphs. At that time, we took care to ensure that members of dSphs or foreground stars did not enter the slit using WINERED's slit viewer, which is sensitive to the R -band ($\lambda_0 = 0.659 \mu\text{m}$) and I -band ($\lambda_0 = 0.800 \mu\text{m}$). The integration time per frame was set to 900 sec for Leo V and 600 sec for Tucana II. The maximum integration time per frame was determined to minimize the effects of (i) saturation from telluric night airglow and (ii) spectral-shifting on the detector due to changes in ambient temperature (Since the slight spectral shifting appeared on the observation in July, we reduced the maximum integration time to 600 sec for the observation in November.) Four frames of Leo V and seven frames of Tucana II were taken with a total exposure time of 3600 sec and 4200 sec, respectively. In order to subtract the components of the telluric lines, and ambient background radiation, such as zodiacal light, sky frames were obtained with the same integration time for each target. The sky regions (one region for Leo V and two regions for Tucana II) were selected to be more than 15 arcmin away from targets in areas without known infrared point sources. Furthermore, for the absolute flux calibration, HD134936 (A0V, $J_m = 9.44$) was observed as the photometric standard star. A0V stars have only a few strong intrinsic absorption lines

from the photosphere in the WINERED wavelength region, making them suitable for use as photometric standard stars in high-resolution spectroscopy. The spectrum of HD134936 was used not only for the flux calibration of Leo V observed on the same night but also for that of Tucana II on a different night. The atmosphere transmittance, $\eta(\lambda)$, is also measured. On the night of November 2nd, the wind was extremely strong, and due to the observatory’s regulations, we were forced to interrupt the observations midway. As a result, we were unable to acquire spectra of the standard star on the November’s run. However, it is known that the efficiency of the WINERED instrument is very stable, and even including variations in atmospheric transmittance, the impact of using a standard star from different nights is not very significant especially for the wavelength regime $\eta(\lambda) \approx 1$. The observation log is shown in Table 1.

Table 1: Observation logs. Here, Regions 1, 2, and 3 are for Leo V, Tucana II, and Tucana II, respectively. R is the spectral resolution. T_I denotes the total integration time.

Object name	Object type	RA(J2000)	DEC(J2000)	Obs. date	J_m	R	T_I (sec)
Leo V	dSph	11:31:09.6	+02:13:12	2023.06.06	–	28,000	3600
Tucana II	dSph	22:51:55.1	-58:34:08	2023.11.02	–	28,000	4200
Sky region 1	–	11:31:56.97	+02:09:19	2023.06.06	–	28,000	1800
Sky region 2	dSph	22:51:06.5	-57:28:46	2023.11.02	–	28,000	1200
Sky region 3	dSph	22:38:08.1	-58:24:39	2023.11.02	–	28,000	1200
HD134936	A0V	15:14:41.4	-52:35:42	2023.06.06	9.44	28,000	90

3.2 Data Reduction

For the data analysis, we utilized the WINERED Automatic Reduction Pipeline (WARP, [39]), provided as the standard pipeline for WINERED. WARP is capable of executing the basic analysis necessary for spectra obtained by WINERED, including sky/scattered light subtraction, flat fielding, interpolation of cosmic-ray-contaminated/bad pixels, transformation of two-dimensional spectra, and wavelength calibration. However, since we found a wavelength shift of approximately 0.1 pixels during a single exposure ($t = 900$ sec) in the raw data of Leo V (even such a small shift can introduce significant systematic errors after sky subtraction due to the peaky profile of airglow lines), we prepared corrected two-dimensional images for the wavelength shifts beforehand and input these data sets into WARP for analysis. By summing up the two-dimensional echelle spectra along the spatial direction (along the slit length) for each order produced by WARP, we finally obtained the average spectrum

$F(\lambda)$ and error spectrum $\sigma(\lambda)$ of the central regions of targets. In conducting flux calibration for the slit spectrometer, it was necessary to estimate the amount of slit loss due to the standard star's image size being wider than the slit width. We estimated the slit loss from the assumption that the stellar image is a Gaussian profile and the seeing size (FWHM) was measured from the spatial-direction cross-section of the two-dimensional spectrum of the standard star on the detector.

3.3 Results

Spectrum-independent analysis We set a 2σ limit on the decay rate of dark matter by requiring the dark matter flux, (7), to be smaller than the reduced spectra in the 2σ range, i.e. $\partial_\Omega \Phi_{\gamma,i} < 2\sigma_i [\frac{4\pi}{m_\phi(1-v_i/c)}] / \eta [\frac{4\pi}{m_\phi(1-v_i/c)}]$, we get the 2σ limit on the decay rate of the dark matter. The combined result is shown in Fig.1,² where the upper panel represents the limit for the decay rate while the lower one is translated into the photon coupling of the ALP dark matter with $q = 2$. In our analysis, we exclusively utilized data where $|F(\lambda)| < 2\sigma(\lambda)$, excluding data points where $|F(\lambda)| > 2\sigma(\lambda)$. This threshold ensures that we consider only data consistent with statistical fluctuations around zero following sky subtraction. Data points exceeding this threshold suggest the presence of non-trivial excesses or systematic errors. Given the potential implications of these excluded data points, we plan to perform further analysis and observations to clarify whether these represent genuine signals or systematic errors. To synthesize the data, we selected the most stringent limits among those derived from the data of Tucana II and Leo V for each bin. Each bin is defined by the range $[m_\phi(1 - 1/28000)^{-1/2} - m_\phi(1 - 1/28000)^{1/2}]$. We varied m_ϕ discretely to cover the whole range from 1.8eV to 2.7eV without overlapping. Thanks to the Doppler shift, the two sets of data can cover most of the range's bins.

We mention that the total observation time for Tucana II is longer than that for Leo V. In addition, the D -factor of the Tucana II can be larger than that of LeoV within the uncertainty range. Therefore, the Tucana II data can set a more stringent constraint. However, there are more Tucana II data to satisfy $|F_i| > 2\sigma_i$, and thus, those data are not considered. The corresponding data may have been affected by adverse weather conditions on the observation date. In such cases, the data from Leo V prove useful, as they provide limits for these bins.

In this analysis, we did not assume the signal to be a line. Therefore, our data can be reinterpreted to also constrain photons in different scenarios, such as multi-body decays of

²The result can be reinterpreted for the scenario where the dark matter is only composed of a fraction r of the total abundance in the dSph, maintaining the same distribution. In this scenario, the vertical axis of the upper panel of Fig.1 can be replaced by $qr\Gamma_\phi$ instead of $q\Gamma_\phi$ without changing the plot [40].

dark matter, dark mediator decays [41], or emissions from dark objects in the dSphs. They can form continuous spectra, which can be constrained using the analysis in this spectrum-independent analysis. We can recast our dark matter limit to apply to scenarios where the spectra originate from cold dark matter or a fraction thereof. This is because, in such cases, the D -factor analysis can be also applied (see, e.g., Ref. [41]).

Since our original data can also be used for different scenarios, which may not relate to the D -factor, we provide the uncertainty of the original data with the zero consistent flux for photon, $2\sigma_i(\lambda)/\eta(\lambda)$, in the supplemental material. Here the atmospheric transmittance η is divided to make the data constrain the photon flux out of the atmosphere.

Analysis for lines We also perform subtraction using a spline fit over each Echelle order by using 20-50 points.³ This method helps to eliminate some systematic errors, particularly under the assumption that the signal conforms to a line spectrum. It allows us to increase the number of bins with photon flux consistent with zero. The resulting limit is illustrated in Fig. 2. This constraint is more stringent than the one presented in Fig. 1, primarily because it incorporates more data from Tucana II. However, unlike the model-independent constraint, this constraint may not be directly applicable to photons with spectra significantly differing from a line. Such spectra might also be inadvertently subtracted due to the specifics of our analysis.

We note that $\mathcal{O}(1)\%$ of the total bins remain unconstrained, where the condition, $|F_i(\frac{4\pi}{m_\phi(1-v_i/c)})| > 2\sigma_i(\frac{4\pi}{m_\phi(1-v_i/c)})$ holds for both for Tucana II and LeoV. These data points will be crucial in our future studies.⁴

4 Conclusions and Discussion

We conducted observations of Leo V and Tucana II using WINERED, installed at the 6.5 m Magellan Clay telescope, for a duration of 1 and 1.2 hours, respectively, in our search for dark matter. By using the data, we have provided the first results of the dark matter search. Our observations and analysis enable us to set one of the strongest limits to date on dark matter decaying into a line photon in the mass range of 1.8 – 2.7 eV.

³This is different from the continuum model analysis in Ref. [19] since we do not subtract the fitted lines.

⁴When applying a constraint derived from a detector with high spectral resolution to line photons of a fixed wavelength, examining the actual data is essential. Subtle features, like vacancies, may not be readily apparent in graphical representations. We provide all the data points for the plots in the supplemental material.

In the data that were not included in the present analysis, we also found excesses of more than 5 sigma local significance by performing a fit-by function of a narrow Gaussian line combined with a smooth spline function. Interestingly, a few of these excesses align between the data from Leo V and Tucana II after accounting for the Doppler shift. This alignment, observed after the Doppler shift analysis, effectively reduces the likelihood that these signals are due to sky emission or imperfect sky subtraction, as the corresponding lines would exhibit shifts between the two targets. However, it must be noted that the observational conditions were not ideal; for example, we experienced strong winds. Therefore, while we observe intriguing excesses, we are cautious about claiming the detection of intrinsic line signals at this stage. Nonetheless, these findings underscore the importance of conducting further observations.

Acknowledgement

W.Y. would like to thank K. Hayashi for the useful discussion on the dark matter profiles. This work was supported by JSPS KAKENHI Grant Nos. 22K14029 (W.Y.), 20H05851 (W.Y.), 21K20364 (W.Y.), and 22H01215 (W.Y.). This paper is based on WINERED data gathered with the 6.5 m Magellan Clay Telescope located at Las Campanas Observatory, Chile, under the proposal "eV-Dark Matter search with WINERED" (PI: Wen Yin, Co-Is: Yuji Ikeda and Taiki Bessho). We thank the staff of Las Campanas Observatory for their support during the WINERED's installation and observations. WINERED was developed by the University of Tokyo and the Laboratory of Infrared High-resolution Spectroscopy, Kyoto Sangyo University, under the financial support of KAKENHI (Nos. 16684001, 20340042, and 21840052) and the MEXT Supported Program for the Strategic Research Foundation at Private Universities (Nos. S0801061 and S1411028). The observing runs in 2023 June and November were partly supported by KAKENHI (grant No. 18H01248), JSPS Bilateral Program Number JPJSBP120239909, and the Project Research Number AB0518 from the Astrobiology Center, NINS, Japan.

References

- [1] R. Daido, F. Takahashi and W. Yin, *The ALP miracle: unified inflaton and dark matter*, *JCAP* **05** (2017) 044 [1702.03284].
- [2] R. Daido, F. Takahashi and W. Yin, *The ALP miracle revisited*, *JHEP* **02** (2018) 104 [1710.11107].

- [3] F. Takahashi and W. Yin, *Hadrophobic Axion from GUT*, 2301.10757.
- [4] S. Chang and K. Choi, *Hadronic axion window and the big bang nucleosynthesis*, *Phys. Lett. B* **316** (1993) 51 [hep-ph/9306216].
- [5] T. Moroi and H. Murayama, *Axionic hot dark matter in the hadronic axion window*, *Phys. Lett. B* **440** (1998) 69 [hep-ph/9804291].
- [6] W. Yin, *Thermal production of cold “hot dark matter” around eV*, *JHEP* **05** (2023) 180 [2301.08735].
- [7] A. Caputo, A. Vittino, N. Fornengo, M. Regis and M. Taoso, *Searching for axion-like particle decay in the near-infrared background: an updated analysis*, *JCAP* **05** (2021) 046 [2012.09179].
- [8] A. Korochkin, A. Neronov and D. Semikoz, *Search for decaying eV-mass axion-like particles using gamma-ray signal from blazars*, *JCAP* **03** (2020) 064 [1911.13291].
- [9] J. L. Bernal, A. Caputo, G. Sato-Polito, J. Mirocha and M. Kamionkowski, *Seeking dark matter with γ -ray attenuation*, *Phys. Rev. D* **107** (2023) 103046 [2208.13794].
- [10] Y. Gong, A. Cooray, K. Mitchell-Wynne, X. Chen, M. Zemcov and J. Smidt, *Axion decay and anisotropy of near-IR extragalactic background light*, *Astrophys. J.* **825** (2016) 104 [1511.01577].
- [11] T. Bessho, Y. Ikeda and W. Yin, *Indirect detection of eV dark matter via infrared spectroscopy*, *Phys. Rev. D* **106** (2022) 095025 [2208.05975].
- [12] W. Yin and K. Hayashi, *Indirect Detection of Decaying Dark Matter with High Angular Resolution: The Case for Axion Search by IRCS on the Subaru Telescope*, *Astrophys. J.* **960** (2024) 98 [2305.13415].
- [13] Y. Ikeda, N. Kobayashi, S. Kondo, C. Yasui, K. Motohara and A. Minami, *Winered: a warm near-infrared high-resolution spectrograph*, in *Ground-Based and Airborne Instrumentation for Astronomy*, vol. 6269, pp. 1224–1231, SPIE, 2006.
- [14] C. Yasui, S. Kondo, Y. Ikeda, A. Minami, K. Motohara and N. Kobayashi, *Warm infrared echelle spectrograph (winered): testing of optical components and performance evaluation of the optical system*, in *Ground-based and Airborne Instrumentation for Astronomy II*, vol. 7014, pp. 1095–1106, SPIE, 2008.
- [15] S. Kondo, Y. Ikeda, N. Kobayashi, C. Yasui, H. Mito, K. Fukue et al., *A warm near-infrared high-resolution spectrograph with very high throughput (winered)*, *arXiv preprint arXiv:1501.03403* (2015) .

- [16] Y. Ikeda, N. Kobayashi, S. Kondo, S. Otsubo, S. Hamano, H. Sameshima et al., *High sensitivity, wide coverage, and high-resolution nir non-cryogenic spectrograph, winered*, in *Ground-based and Airborne Instrumentation for Astronomy VI*, vol. 9908, pp. 1800–1813, SPIE, 2016.
- [17] Y. Ikeda, N. Kobayashi, S. Kondo, S. Otsubo, A. Watase, T. Murai et al., *Very high-sensitive nir high-resolution spectrograph winered: on-going observations at ntt*, in *Ground-based and Airborne Instrumentation for Astronomy VII*, vol. 10702, pp. 1751–1762, SPIE, 2018.
- [18] Y. Ikeda, S. Kondo, S. Otsubo, S. Hamano, C. Yasui, N. Matsunaga et al., *Highly Sensitive, Non-cryogenic NIR High-resolution Spectrograph, WINERED*, *pasp* **134** (2022) 015004.
- [19] R. Janish and E. Pinetti, *Hunting Dark Matter Lines in the Infrared Background with the James Webb Space Telescope*, 2310.15395.
- [20] S. Roy, C. Blanco, C. Dessert, A. Prabhu and T. Temim, *Sensitivity of JWST to eV-Scale Decaying Axion Dark Matter*, 2311.04987.
- [21] D. Grin, G. Covone, J.-P. Kneib, M. Kamionkowski, A. Blain and E. Jullo, *A Telescope Search for Decaying Relic Axions*, *Phys. Rev. D* **75** (2007) 105018 [astro-ph/0611502].
- [22] M. Regis, M. Taoso, D. Vaz, J. Brinchmann, S. L. Zoutendijk, N. F. Bouché et al., *Searching for light in the darkness: Bounds on ALP dark matter with the optical MUSE-faint survey*, *Phys. Lett. B* **814** (2021) 136075 [2009.01310].
- [23] E. Todarello, M. Regis, J. Reynoso-Cordova, M. Taoso, D. Vaz, J. Brinchmann et al., *Robust bounds on ALP dark matter from dwarf spheroidal galaxies in the optical MUSE-Faint survey*, 2307.07403.
- [24] M. Wenger et al., *The simbad astronomical database*, *Astron. Astrophys. Suppl. Ser.* **143** (2000) 9 [astro-ph/0002110].
- [25] C. Combet, D. Maurin, E. Nezri, E. Pointecouteau, J. A. Hinton and R. White, *Decaying dark matter: a stacking analysis of galaxy clusters to improve on current limits*, *Phys. Rev. D* **85** (2012) 063517 [1203.1164].
- [26] A. Geringer-Sameth, S. M. Koushiappas and M. Walker, *Dwarf galaxy annihilation and decay emission profiles for dark matter experiments*, *Astrophys. J.* **801** (2015) 74 [1408.0002].

- [27] V. Bonnavard et al., *Dark matter annihilation and decay in dwarf spheroidal galaxies: The classical and ultrafaint dSphs*, *Mon. Not. Roy. Astron. Soc.* **453** (2015) 849 [1504.02048].
- [28] V. Bonnavard, C. Combet, D. Maurin, A. Geringer-Sameth, S. M. Koushiappas, M. G. Walker et al., *Dark matter annihilation and decay profiles for the Reticulum II dwarf spheroidal galaxy*, *Astrophys. J. Lett.* **808** (2015) L36 [1504.03309].
- [29] K. Hayashi, K. Ichikawa, S. Matsumoto, M. Ibe, M. N. Ishigaki and H. Sugai, *Dark matter annihilation and decay from non-spherical dark halos in galactic dwarf satellites*, *Mon. Not. Roy. Astron. Soc.* **461** (2016) 2914 [1603.08046].
- [30] J. L. Sanders, N. W. Evans, A. Geringer-Sameth and W. Dehnen, *Indirect Dark Matter Detection for Flattened Dwarf Galaxies*, *Phys. Rev. D* **94** (2016) 063521 [1604.05493].
- [31] N. W. Evans, J. L. Sanders and A. Geringer-Sameth, *Simple J-Factors and D-Factors for Indirect Dark Matter Detection*, *Phys. Rev. D* **93** (2016) 103512 [1604.05599].
- [32] K. Hayashi, M. Fabrizio, E. L. Lokas, G. Bono, M. Monelli, M. Dall’Ora et al., *Dark halo structure in the Carina dwarf spheroidal galaxy: joint analysis of multiple stellar components*, *Mon. Not. Roy. Astron. Soc.* **481** (2018) 250 [1804.01739].
- [33] M. Petac, P. Ullio and M. Valli, *On velocity-dependent dark matter annihilations in dwarf satellites*, *JCAP* **12** (2018) 039 [1804.05052].
- [34] K. Hayashi, M. Chiba and T. Ishiyama, *Diversity of Dark Matter Density Profiles in the Galactic Dwarf Spheroidal Satellites*, *Astrophys. J.* **904** (2020) 45 [2007.13780].
- [35] K. Hayashi, Y. Hirai, M. Chiba and T. Ishiyama, *Dark Matter Halo Properties of the Galactic Dwarf Satellites: Implication for Chemo-dynamical Evolution of the Satellites and a Challenge to Lambda Cold Dark Matter*, *Astrophys. J.* **953** (2023) 185 [2206.02821].
- [36] A. Smette, H. Sana, S. Noll, H. Horst, W. Kausch, S. Kimeswenger et al., *Molecfit: A general tool for telluric absorption correction-i. method and application to eso instruments*, *Astronomy & Astrophysics* **576** (2015) A77.
- [37] W. Kausch, S. Noll, A. Smette, S. Kimeswenger, M. Barden, C. Szyszka et al., *Molecfit: A general tool for telluric absorption correction-ii. quantitative evaluation on eso-ult/x-shooterspectra*, *Astronomy & Astrophysics* **576** (2015) A78.
- [38] Y. Ikeda, S. Kondo, S. Otsubo, S. Hamano, C. Yasui, N. Matsunaga et al., *Highly Sensitive, Non-cryogenic NIR High-resolution Spectrograph, WINERED, pasp* **134** (2022) 015004.

- [39] S. Hamano, Y. Ikeda, S. Otsubo, H. Katoh, K. Fukue, N. Matsunaga et al., *Warp: The data reduction pipeline for the winered spectrograph*, *Publications of the Astronomical Society of the Pacific* **136** (2024) 014504.
- [40] K. Nakayama and W. Yin, *Anisotropic cosmic optical background bound for decaying dark matter in light of the LORRI anomaly*, 2205.01079.
- [41] J. Jaeckel and W. Yin, *Shining ALP dark radiation*, *Phys. Rev. D* **105** (2022) 115003 [2110.03692].

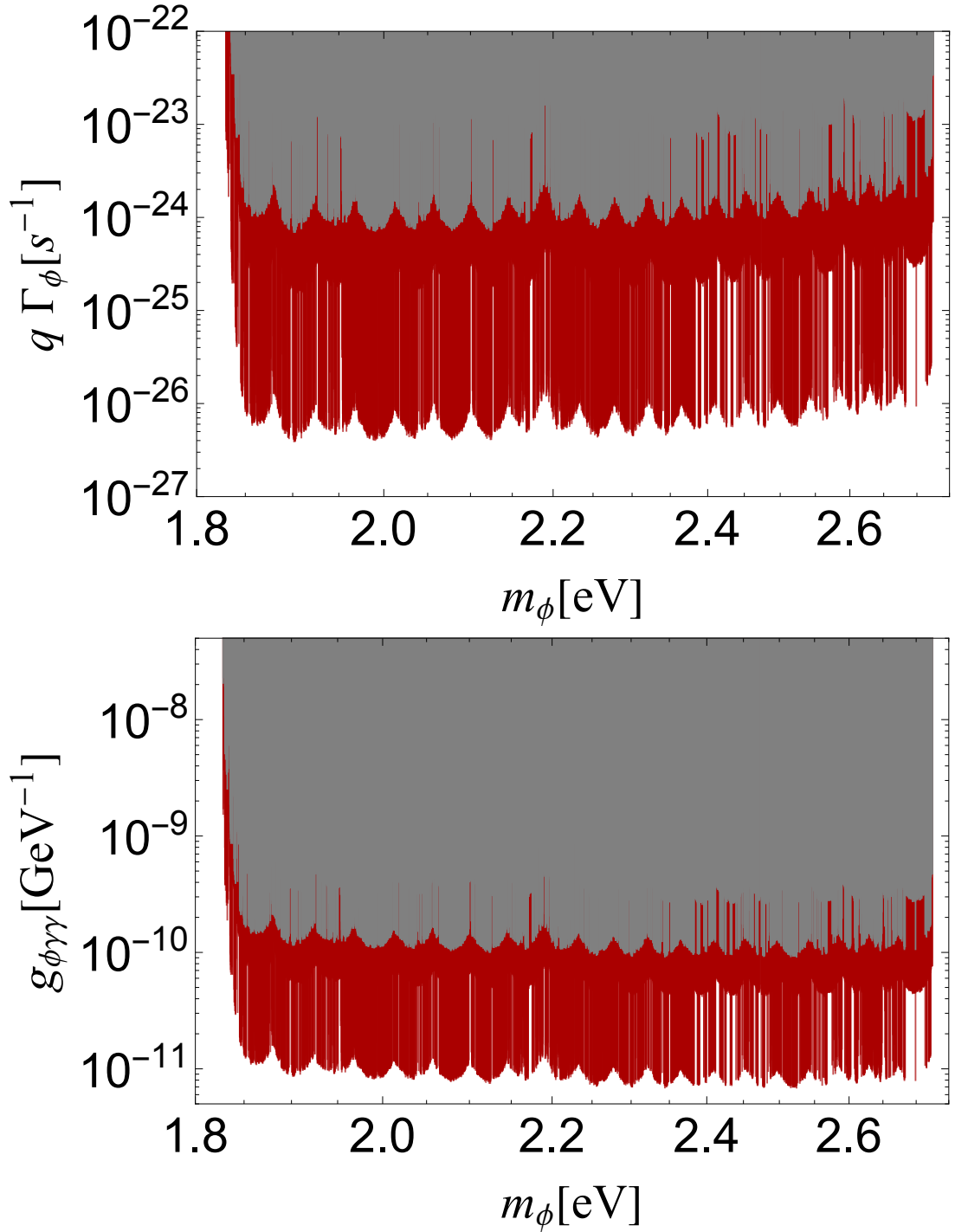


Figure 1: 2σ limit for dark matter decay into two massless particles, one of which is a photon. The top panels show the constraints on the decay rate multiplied by the number of photons in the final state, q , by varying the mass m_ϕ . The red band corresponds to the theoretical uncertainty in the differential D -factor. The bottom panels display the translated constraints on the photon coupling, $g_{\phi\gamma\gamma}$, for the ALP dark matter ($q = 2$).

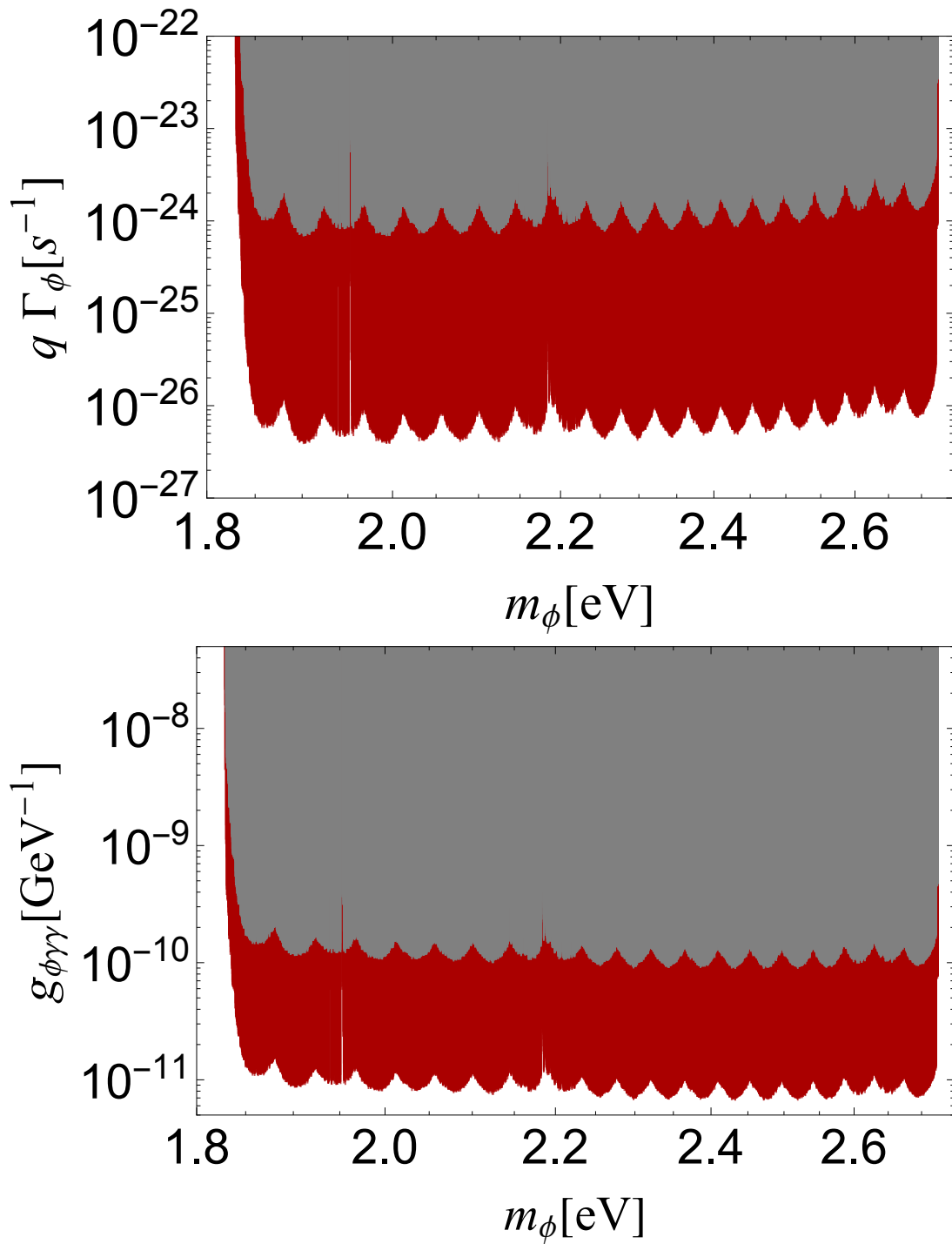


Figure 2: Same as Fig.1, but we subtract the excesses of the continuum spectra to increase viable bins for constraining the line photons.